JOURNAL OF GEOPHYSICAL RESEARCH, VOL. 102, NO. D9, PAGES 10,815–10,828, MAY 20, 1997

Ozone depletion in the late winter lower Arctic stratosphere: Observations and model results

A. Bregman,[1] M. van den Broek,[2] K. S. Carslaw,[3] R. Müller,[4]
T. Peter,[3] M. P. Scheele,[5] and J. Lelieveld[1]

Abstract. Ozone loss rates in the lowermost part of the Arctic stratosphere (at potential temperature levels ≤375 K) in the period January and February 1993 are calculated using a chemistry-trajectory model and 30-day back trajectories. The results were compared with observations carried out during the first Stratosphere Troposphere Experiment by Aircraft Measurements (STREAM) in February 1993 in the Arctic lower stratosphere. Relatively low N_2O and low O_3 concentrations were measured during STREAM, and O_3 loss rates of 8.0 (±3.6) ppbv d^{-1} were calculated from O_3-N_2O STREAM data in the vortex area. The average O_3 loss rate calculated by the model is 8.6 ppbv d^{-1} (1.3% d^{-1}), in agreement with observations. However, the calculated O_3 loss rate decreases to the lower value of the observed loss rates when taking into account N_2O-Cl_y interrelations from different studies. Heterogeneous reactions on liquid sulfuric acid aerosols, in particular those involving the chlorine reservoir species $ClONO_2$ and HCl, must be considered to explain the observed O_3 loss rates. Complete conversion of $ClONO_2$ and HCl to active chlorine by heterogeneous reactions in the model occurs at temperatures ≤205 K under conditions with enhanced aerosol loading, and at temperatures ≤200 K with background aerosol levels. Since the trajectory temperatures were frequently below 205 K and occasionally below 200 K, the model results are (1) sensitive to the Cl_y level but relatively insensitive to the initial chlorine partitioning within Cl_y and (2) show significant O_3 loss at background aerosol levels, being only 1–2 ppbv d^{-1} less compared to conditions with enhanced aerosol loading. We conclude that future O_3 loss in the Arctic lower stratosphere is quite sensitive to temperature changes, while it appears to be less sensitive to enhanced aerosol loading (e.g., by volcanic sulfate particles).

1. Introduction

Recent eruptions of El Chichon and Mount Pinatubo temporarily enhanced the sulfate aerosol mass in the stratosphere down to the tropopause by factors of 10–100 [*Trepte et al.*, 1993]. Model studies of the post-Pinatubo high-latitude winter lower Arctic stratosphere generally indicate enhanced O_3 losses due to heterogeneous reactions on the increased sulfuric acid aerosol [e.g., *Lefèvre et al.*, 1994; *Tie et al.*, 1994; *Granier and Brasseur*, 1992; *Brasseur and Granier*, 1992; *Pitari and Rizi*, 1993; *Rodriguez et al.*, 1991, 1994; *Chipperfield et al.*, 1995]. The liquid state of the aerosols can play a more important role in O_3 loss than previously assumed because of the low freezing probabilities below nitric acid trihydrate (NAT) formation threshold temperatures (193–195 K) [*Drdla et al.*, 1994; *Carslaw et al.*, 1994; *Tabazadeh et al.*, 1994]. O_3 depletion in the lower part of the high-latitude winter stratosphere (i.e., below about 17 km altitude, in the following referred to as "lowermost stratosphere") is of special concern due to its potential contribution to the observed negative trend in O_3 at northern middle latitudes [*World Meteorological Organization* (*WMO*), 1994], which is also found by modeling studies of the 1991–1992 Arctic winter [*Lefèvre et al.*, 1994]. However, recent studies concluded that southward transport of O_3-poor vortex air cannot fully account for the observed middle-latitude O_3 loss in 1993 [*Shindell et al.*, 1994; *Jones and MacKenzie*, 1995].

O_3 loss in the lowermost winter stratosphere is significantly enhanced by formation of Cl_2 through heterogeneous reactions and subsequent photolysis of Cl_2 into active chlorine. In this part of the Arctic stratosphere, liquid aerosols are mainly involved in heterogeneous processing, since temperatures are generally higher than 195 K, which is above the threshold temperatures of the existence of solid nitric acid hydrates. The zonally averaged polar stratospheric cloud (PSC) formation probability in this part of the stratosphere is less than 4% [*Poole and Pitts*, 1994]. HCl solubility increases with decreasing temperature, and below ~200 K is sufficiently soluble to lead to an enhanced chlorine activation rate, even at background aerosol loading [*Hanson et al.*, 1994; *Carslaw*, 1994; *Hanson and Ravishankara*, 1993; *Luo et al.*, 1994]. The lowermost stratosphere in the 1992–1993 winter is very interesting in this respect, since this winter was characterized by unusually low temperatures in the lower stratosphere compared to previous winters [*National Oceanic and Atmospheric Administration* (*NOAA*), 1993]. In addition, the lower stratospheric vortex air was particularly well isolated, indicated by an unusually strong potential vorticity (PV) gradient compared to the prior 16 Arctic winters, associated with the presence of a relatively

[1]Institute for Marine and Atmospheric Research Utrecht, Utrecht, Netherlands.
[2]Space Research Organisation of the Netherlands, Utrecht.
[3]Max Planck Institute for Chemistry, Mainz, Germany.
[4]Atmospheric Chemistry Department Jülich GmbH, Jülich, Germany.
[5]Royal Netherlands Meteorological Institute, De Bilt, Netherlands.

Paper number 97JD00006.
0148-0227/97/97JD-00006$09.00

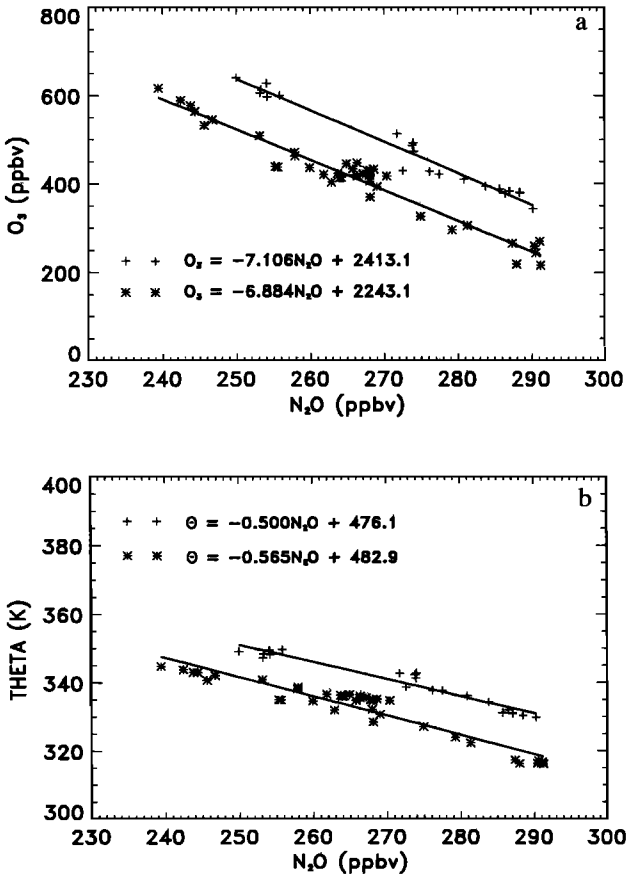

Figure 1. N_2O, O_3 (parts per billion by volume) (a) and θ (kelvins) (b) data for February 16, and 18, 1993 (pluses) and February 17 only (stars). The solid lines represent the fitting vectors.

strong polar night jet [*Manney et al.*, 1994a, b, 1995; *Dahlberg and Bowman*, 1995]. Moreover, enhanced sulfuric acid aerosol loading from the eruption of Mount Pinatubo was still present, and significantly higher concentrations of active chlorine species were found during late winter in the lower part of the stratosphere [*Manney et al.*, 1994c; *Shindell et al.*, 1994] compared to the previous winter [*Waters et al.*, 1993; *Toohey et al.*, 1993] and the subsequent winter [*Waters et al.*, 1995]. In fact, record low O_3 concentrations have been measured during winter and early spring 1993 in the lower stratosphere at middle and high northern latitudes [e.g., *Kerr et al.*, 1993; *Bojkov et al.*, 1993; *Komhyr et al.*, 1994; *Randel et al.*, 1995; *Müller et al.*, 1996].

Estimates of O_3 depletion in the lowermost stratosphere at high northern latitudes during this winter are rare. Loss rates of 1.1–1.7% d^{-1} between the 450 and 380 K potential temperature (θ) levels (approximate altitude 16–20 km) were calculated based on aerosol and O_3 profiles obtained from balloon soundings at high northern latitudes during January and February 1993 [*Larsen et al.*, 1994]. These results agree with O_3 depletion rates for the same period derived from the first Stratosphere Troposphere Experiment by Aircraft Measurements (STREAM I) N_2O and O_3 aircraft measurements (1.2% or 7 ppbv day^{-1} at θ = 350 K) [*Bregman et al.*, 1995], although the estimates by Larsen et al. at the 380 K level are somewhat higher. Similar depletion rates were estimated for the lower stratosphere at θ levels ≥400 K for January and February 1992 [*Proffitt et al.*, 1993], for January–March 1992 [*Braathen et al.*, 1994], and for February 1989 [*McKenna et al.*, 1990].

Here, a chemistry-trajectory model is used to calculate O_3 loss rates in the lowermost Arctic stratosphere during January–February 1993. The results are compared with observed O_3 loss rates derived from the STREAM I data. Further, we discuss uncertainties associated with initialization and assumed model parameters.

2. Ozone Loss Rates Derived From the STREAM I Data

During the STREAM I project simultaneous in situ measurements of O_3, N_2O, and HNO_3 were carried out on board a Dutch Cessna Citation II twin engine jet aircraft. The measurements were performed in the afternoon on February 16, 17, and 18, 1993, up to 13 km (pressure altitude approximately 160 hPa) between 68°–74°N with Kiruna airport as operation base. The results from three flights have been analyzed and described previously [*Bregman et al.*, 1995]. Relatively low N_2O concentrations were measured during all flights down to 230 ppbv at the 350 K potential temperature level and potential vorticity values ≥10 PVU (PVU = K kg^{-1} m^2 s^{-1}), indicating that the aircraft flew in the stratosphere. Many of the calculated 10-day back trajectories followed the vortex edge at 150 hPa, suggesting that vortex air was present at flight altitudes. These air parcels have been selected in Figure 1a, showing 1-min averaged N_2O-O_3 data. The prewinter relationships measured in 1988 and 1991 during the Airborne Arctic Stratospheric Experiment (AASE) I and II [*Proffitt et al.*, 1990; *Collins et al.*, 1993] show significantly higher O_3 mixing ratios relative to N_2O, compared with the STREAM results, indicating that photochemical loss of O_3 occurred during descent inside the polar vortex area in the air parcels measured during STREAM. The chemical lifetimes of both species are sufficiently long compared to dynamic timescales to cause a strong anticorrelation in the lower stratosphere [e.g., *Brasseur and Solomon*, 1986]. Since the chemical lifetime of N_2O in this part of the stratosphere is more than 100 years, it can be regarded as a conservative quantity, and a change in the slope of the O_3-N_2O relation can be explained by enhanced photochemical loss of O_3 [*Plumb and Ko*, 1992]. Hence O_3 decreases relative to N_2O during the winter inside the vortex, and since polar vortex air becomes relatively isolated from midlatitude air, the slope of the O_3-N_2O relation deviates from the prewinter relationship.

The STREAM results are separated into two different parts with comparable slopes, which are shown in Figure 1a. The two relations represent data measured on February 17 (stars) and February 16 and 18 (pluses, see also *Bregman et al.* [1995, Figure 10]). Although both relations show that the air is chemically processed, the data on February 17 suggest chemical processing for a longer time. The time difference between these two relations can be estimated from the STREAM I N_2O-θ relations. Polar vortex air deviates more from radiative equilibrium than midlatitude air during the winter and thus shows stronger diabatic cooling [*Schoeberl et al.*, 1992; *Manney et al.*, 1994b], while N_2O mixing ratios remain unchanged. Thus inner vortex air contains lower N_2O mixing ratios than extravortex air on the same θ level. Using the N_2O-θ relations in Figure 1b, this difference in N_2O concentration can be translated into a difference in θ. The air with the lowest O_3 concentrations relative to N_2O (lower line, February 17) has θ values

which are 8–15 K lower than those on February 16 and 18. Assuming that cross-vortex boundary transport is isentropic, the air on February 17 presumably spent more time inside the vortex than the air on February 16 and 18. On the basis of diabatic cooling rates for the winter 1992–1993 [*Larsen et al.*, 1994; *Manney et al.*, 1994b], the differences in θ correspond to a time difference of 15–22 days. This is equivalent to an O_3 loss rate of 8.0 ($\pm$3.6) ppbv d^{-1} for N_2O concentrations of 240 ppbv. This agrees with the loss rates estimated by *Bregman et al.* [1995], which were calculated for February 17 and 18 only. The method applied to calculate the O_3 loss rates and the root-mean-square errors is described in the appendix.

3. Model Description

The model was originally developed to simulate the chemistry of the high-latitude winter stratosphere [*Müller and Crutzen*, 1993; *Müller et al.*, 1994; *Crutzen et al.*, 1992]. The chemical scheme for gas phase chemistry involves 55 bimolecular, 13 termolecular, and 22 photolysis reactions. The model uses a Gear method to numerically integrate the coupled set of stiff differential equations. Photolysis rates are calculated with a radiative transfer model [*Lary and Pyle*, 1991], which has been recently updated (D. J. Lary, private communication, 1995), and which includes the temperature dependence of the UV cross sections for HNO_3 [*Burkholder et al.*, 1993] and the parametrization of the $O(^1D)$ quantum yield from the O_3 photolysis for $300 < \lambda < 325$ nm [*Michelsen et al.*, 1994]. Ternary and binary gas phase reaction rate coefficients are taken from *DeMore et al.* [1994]. The model includes the following heterogeneous reactions on liquid particles:

$$N_2O_5 + H_2O \rightarrow 2HNO_3 \quad (1)$$

$$ClONO_2 + H_2O \rightarrow HOCl + HNO_3 \quad (2)$$

$$ClONO_2 + HCl \rightarrow Cl_2 + HNO_3 \quad (3)$$

$$HOCl + HCl \rightarrow Cl_2 + H_2O \quad (4)$$

The composition and volume of liquid $HNO_3/H_2SO_4/H_2O$ aerosols are calculated using the analytic expression of *Carslaw et al.* [1995a], based on the thermodynamic model of *Carslaw et al.* [1995b]. The solubility of HCl is calculated using the fitting equations of *Luo et al.* [1994], and that of HOCl from *Huthwelker et al.* [1995].

The reactive uptake coefficients (fraction of molecules lost due to reaction upon collision with surface, γ) for (2) and (3) were taken from the parametrization of *Hanson and Ravishankara* [1994], which accounts for the competition between (2) and (3).

For N_2O_5 hydrolysis (reaction (1)) we assume $\gamma = 0.1$. *Fried et al.* [1994] did not find a significant particle size dependence of γ, and derived values of 0.077 for 60 wt% H_2SO_4 to 0.146 for 70 wt% H_2SO_4 at temperatures of 230 K, in agreement with recent laboratory experiments by *Hanson and Lovejoy* [1994].

For (4) we use the expressions given by *Hanson and Ravishankara* [1994], except that we use an HOCl liquid phase diffusivity and Henry's law constant, H^*_{HOCl} from *Huthwelker et al.* [1995]. We also include an additional term describing the reaction between HCl and the HOCl that is produced in the droplet from (2) [*Carslaw*, 1994].

4. Back Trajectory Calculations and Initialization

Back Trajectories

The ECMWF (European Centre for Medium-Range Weather Forecasts) three-dimensional (3-D) wind field high-resolution analyses (~0.5° latitude/longitude and 31 vertical layers) have been used to calculate 30-day back trajectories, including diabatic effects. The wind fields were updated every 3 hours. The period of 30 days covers the time period of the observed O_3 loss rates. The uncertainties in the trajectory temperatures, pressures, and location of the air parcels increase with increasing integration time, and thus caution is warranted, especially during the initial part of the 30-day back trajectories. Therefore we have used 60 trajectories starting at different flight levels down to the 185 hPa pressure level for the three flights carried out during the STREAM I campaign [*Bregman et al.*, 1995]. All trajectories (not shown) show approximately the same variations in latitude, longitude, pressure, and temperature, and they follow the vortex edge at 150 hPa closely. A total of 21 trajectories started at the highest flight level (160 hPa) of the STREAM I flight on February 17, 1993, and have been used for the model calculations in this study. Figures 2a–2d show the temperature, potential temperature, pressure, and solar zenith angles of these 21 trajectories. The 30-day average diabatic cooling rate is 0.5 K day^{-1} (with 1σ = 0.2 K), which agrees with previous estimates for the 1992–1993 winter [*Manney et al.*, 1994b; *Larsen et al.*, 1994]. The longitudinal and latitudinal variations of 10 trajectories, being typical for all 21 trajectories, are depicted in Figure 3. It can be seen that the trajectories closely follow the vortex edge at 150 hPa on January 17 and February 17, 1993 (Figures 4a and 4b), where the location of the vortex edge is represented by the large gradient in geopotential heights. In addition, the vortex structure on the 50 hPa level [*Bregman et al.*, 1995] is comparable to that at 150 hPa, illustrating that the vortex was strongly developed over a wide range of altitudes during the 1992–1993 winter, as mentioned earlier. Moreover, the location of the vortex in Figures 4a and 4b agrees well with the representation of the Arctic polar vortex at θ = 465 K during January and February 1993 derived from temperature, aerosol extinction coefficients, and $ClONO_2$ data of the cryogenic limb array etalon spectrometer (CLAES) experiment on board the UARS satellite [*Roche et al.*, 1994].

Trajectory Model Initialization

Table 1 summarizes the initialization of chemical species for the model simulations.

Ozone. There are no O_3 data available to initialize the model. Initial O_3 concentrations were calculated from O_3 loss rates derived from the STREAM I measurements multiplied by the number of simulated days (30) and added to the O_3 concentrations of the air parcels on the flight track where the trajectories end. Note that we are only interested in changes in O_3, and not in absolute mixing ratios. We further "updated" the initial O_3 levels each time changes were made in the model.

Chlorine species. The N_2O concentrations measured during STREAM I were used to obtain Cl_y mixing ratios from the empirical N_2O-Cl_y relation for high northern latitudes [*Woodbridge et al.*, 1995] and resulted in 1200–1700 pptv Cl_y for 240 ppbv N_2O. Woodbridge et al. derived Cl_y from the difference between estimated total chlorine and measured total organic chlorine abundance. The range refers to the 5% uncertainty in

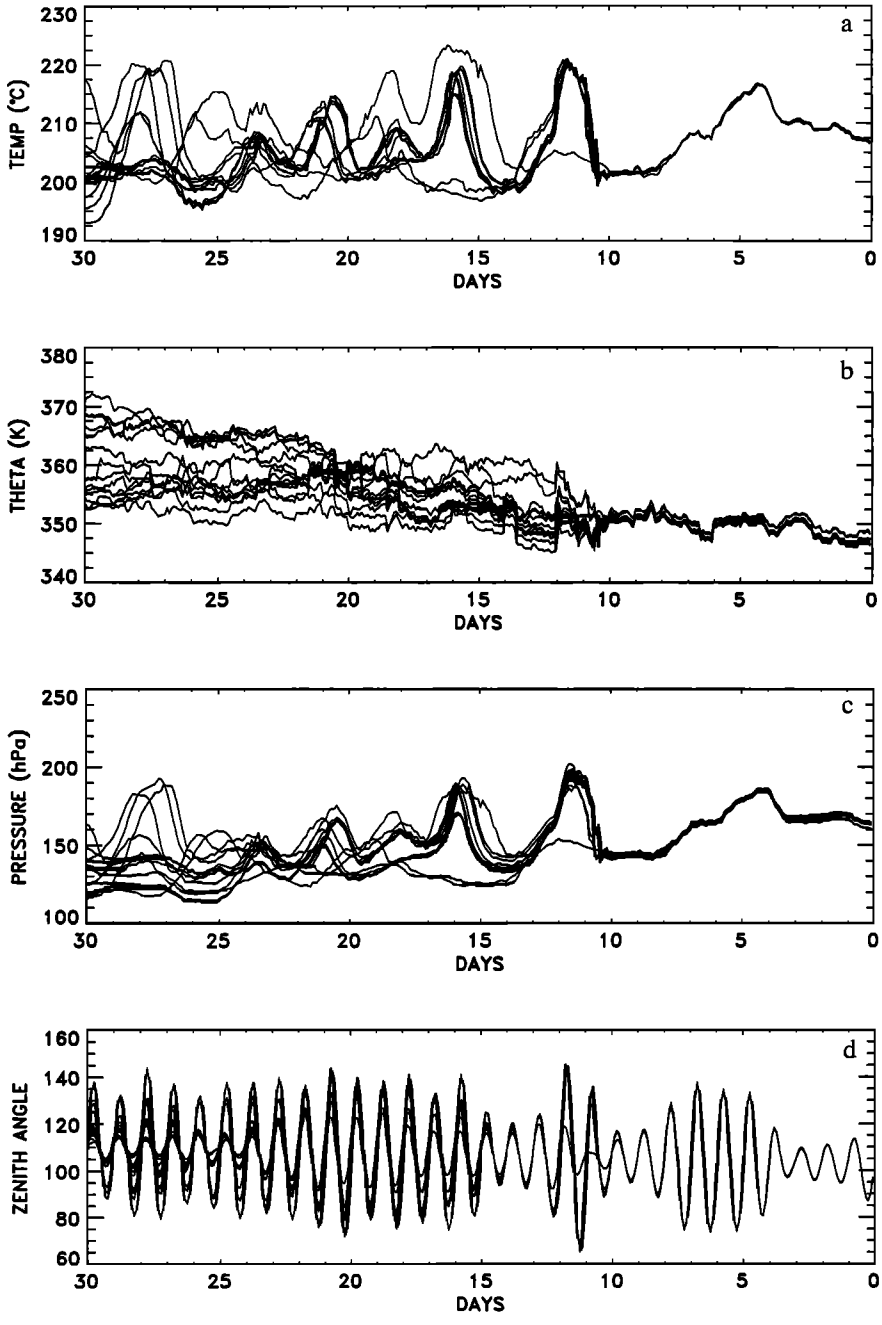

Figure 2. (a) Trajectory temperature, (b) potential temperature, in kelvins, (c) pressure, and (d) zenith angles of the twenty-one 30-day back trajectories.

the calculated total chlorine. Lower Cl_y concentrations were derived from other observations and are discussed in section 6. The initial partitioning within Cl_y is complicated by its high variability during the winter. The two most important chlorine reservoir species, HCl and $ClONO_2$, can be converted rapidly into active chlorine species through heterogeneous reactions during the winter, as has been shown by observations and model simulations for the 1991–1992 and 1992–1993 winters [e.g., *Webster et al.*, 1993; *Müller et al.*, 1994; *von Clarmann et al.*, 1993, 1995; *Müller et al.*, 1996; *Notholt et al.*, 1995; *Blom et al.*, 1995; *Chipperfield et al.*, 1995]. Although $ClONO_2$ could dominate over HCl during the polar night [*Webster et al.*, 1993], balloon measurements at high latitudes in January 1992 showed low $ClONO_2$ concentrations (less than 100 pptv) in the lower stratosphere, comparable to the reduced HCl levels [*von Clarmann et al.*, 1993, 1995]. However, large uncertainties in the measurements exist at $\theta < 400$ K. Considering the uncertainties in the measurements, the simulations were initialized with 50% active (in the form of HOCl and Cl_2O_2) and 50% reservoir species (in the form of $ClONO_2$ and HCl). Sensitivity tests were performed to investigate the effect of different initial fractions of active and reservoir chlorine species on O_3 depletion rates (section 6).

Nitrogen species. Initial HNO_3 concentrations were adjusted so that the concentrations after 30 days agreed with the STREAM data at 160 hPa on February 17 (3.5 ppbv) [*Bregman*

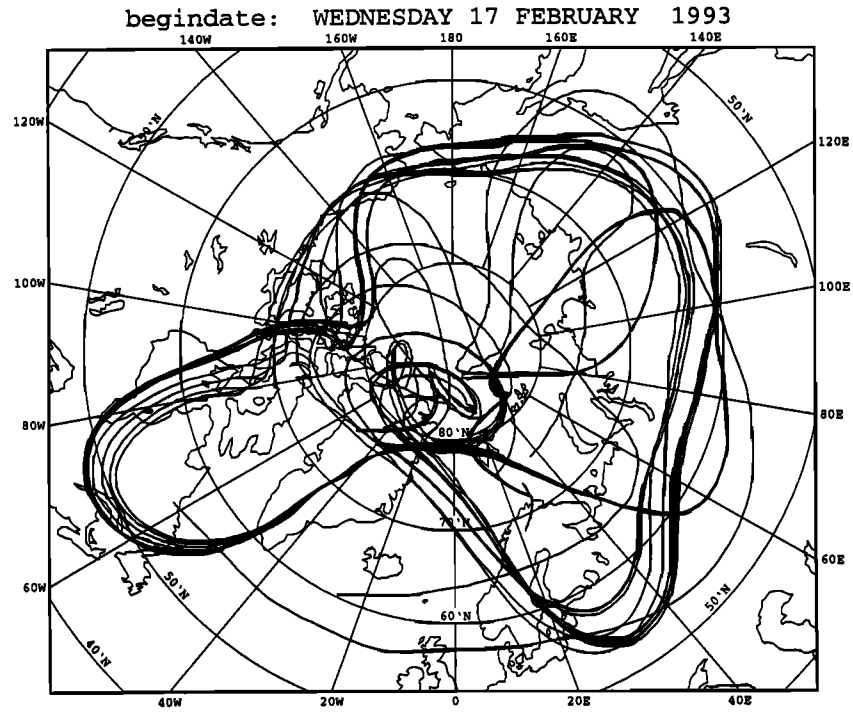

Figure 3. Longitude and latitude variation of the selected 30-day back trajectories, starting on the highest flight level on February 17, 1993 (see text for details). The solid line represents the flight track.

et al., 1995]. HNO_3 increases through heterogeneous conversion of N_2O_5 and $ClONO_2$ (reactions (1) and (2)), however, by a relatively small amount since the concentrations of these species together are less than ~500 pptv in the lowermost stratosphere, compared to typically 4–5 ppbv [*Bregman et al.*, 1995]. Initial N_2O_5 and NO_x (= NO + NO_2 + NO_3) mixing ratios were obtained from the Mainz two-dimensional (2-D) model of the stratosphere. Similar calculations were carried out for earlier winters [*Brühl and Crutzen*, 1993].

Bromine species. Data for BrO in the winter lower stratosphere are limited, and there have been no measurements performed during the 1992–1993 winter (see *WMO* [1994] for an overview). Recent measurements of source gases of BrO_x radicals in the 1991–1992 winter indicated concentrations of

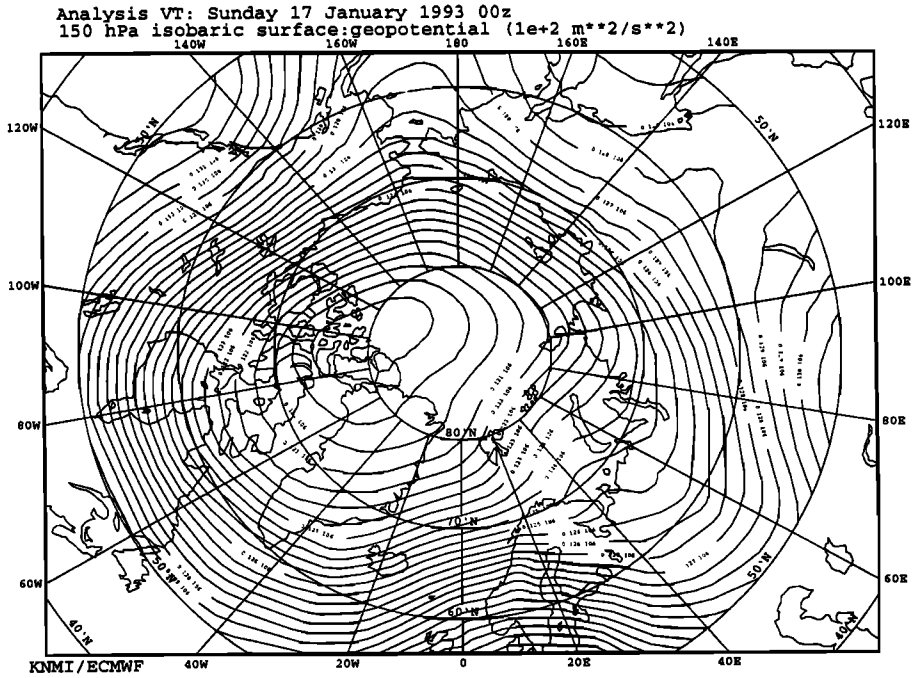

Figure 4a. ECMWF analyses of the geopotential heights ($m^2\ s^{-2}$) at 150 hPa on January 17. The flight track is indicated with the solid line.

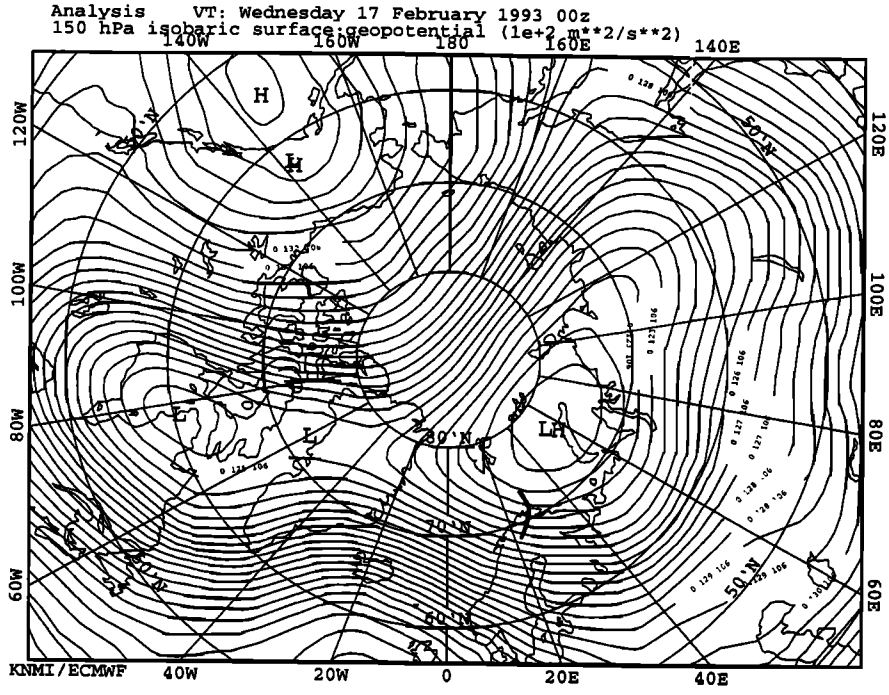

Figure 4b. ECMWF analyses of the geopotential heights ($1e + 2$ m^2 s^{-2}) at 150 hPa on February 17.

close to zero at the tropopause and up to 11.4 pptv at 19 km altitude [*Fabian et al.*, 1994]. In situ measurements during the second Airborne Arctic Stratospheric Experiment (AASE II) in the Arctic vortex in 1992 showed BrO concentrations of 3–7 pptv at the 400 K potential temperature level (~18 km altitude) [*Avallone et al.*, 1995], comparable to the results of AASE I in 1989 [*Toohey et al.*, 1990]. Since the trajectories used in this study all originate from altitudes of 12–16 km (330–380 K), the simulations were initialized with BrO mixing ratios of 5 pptv, assuming that all initial inorganic bromine is BrO. The calculated BrO noontime concentrations are 2.5–3.5 pptv.

Aerosols. The aerosol loading in the Arctic vortex during the winter 1992–1993 was still enhanced in the lower stratosphere due to the eruption of Mount Pinatubo in 1991. Especially in the lower part of the Arctic stratosphere the aerosol loading was more enhanced than in the previous winter, probably due to the development of the polar vortex in 1991 before the Pinatubo aerosol was transported to the Arctic [*Stone et al.*, 1993; *Rosen et al.*, 1994; *Browell et al.*, 1993], and partly due to the movement of peak aerosol concentrations to lower altitudes by gravitational settling, as has been found at northern midlatitudes [*Deshler et al.*, 1993]. Balloon measurements in the Arctic stratosphere during February 1993 showed a particle number density of about 10 cm^{-3} and a surface area of 15–20 μm^2 cm^{-3} [*Deshler and Oltmans*, 1997]. A unimodal lognormal aerosol distribution is assumed, and a mode radius of 0.25 μm has been calculated from the width of the aerosol distribution, number density, and total volume representative of Mount Pinatubo conditions in the Arctic vortex [*Pueschel et al.*, 1994; *Deshler et al.*, 1993; *Deschler and Oltmans*, 1997].

For the sensitivity study, background aerosol concentrations (~0.5 cm^{-3}) and surface areas (~1 μm^2 cm^{-3}), typical for the lower stratosphere, were taken from *Deshler et al.* [1993].

5. Results

Back Trajectories on February 17

Figure 5 shows O_3 loss rates derived from the STREAM I data by *Bregman et al.* [1995], and the results of the 30-day model simulations using all 21 back trajectories. The calculated average O_3 loss rate is 8.6 ppbv d^{-1} (1.3% d^{-1}) for 30 days, with a standard deviation (σ) of 7%, which is close to the observed O_3 loss rate from the STREAM I data.

We use trajectory 16 (since this trajectory yields an O_3 loss rate closest to the averaged loss rate of all 21 trajectories, see Figure 5) to illustrate the effect of variation in concentrations of relevant chemical species, temperature, zenith angle, and other important variables on O_3 loss rates. Figures 6a–6d depict the time series of trajectory temperature, pressure, latitude, and solar zenith angle. The air parcel reaches relatively low latitudes (50°–55°N) with minimum solar zenith angles of

Table 1. Initialization of the Model Simulations

Species	Value, ppbv
O_3	850
CH_4	1400
CO	25
N_2O	240
H_2O	4000
H_2	560
HNO_3	3.0
NO_x (= HNO_4 + 2 × N_2O_5 + NO + NO_2)	0.05
HCl	0.36
$ClONO_2$	0.36
HOCl	0.36
Cl_2O_2	0.36
BrO	0.005
CH_2O	0.08
CH_3O_2H	0.025

65°–70° during two periods, corresponding to the low-pressure regions above northern Greenland and Novaya Zemlya. The temperature varies significantly and is occasionally below 200 K.

The surface areas of the liquid aerosols and the sulfuric acid weight percent are shown in Figure 7. After a few days the sulfuric acid weight fraction decreases significantly due to the relatively low temperatures, and nearly complete heterogeneous removal of HCl and $ClONO_2$ (Figure 8) occurs. Although the temperatures are relatively low, they are still too high with respect to HNO_3 solubility in the liquid aerosols [*Carslaw et al.*, 1995b], so the HNO_3 weight fractions are negligible.

Figure 8 also shows that at temperatures close to or below 200 K the first-order loss rate of HCl is faster than that of $ClONO_2$. This is due to the reaction HOCl + HCl and the fact that the availability of HOCl (initially 360 pptv) is not limited by its formation from (2). In addition, the reactive uptake coefficient of (4) is higher than that of (2) at these temperature and pressure levels, so the first-order rate coefficient of (4) is 2–3 orders of magnitude larger than that of (2). When the temperature increases, a significant increase of HCl and $ClONO_2$ in the gas phase occurs. For HCl this is mainly due to the reaction of Cl with CH_4, and for $ClONO_2$ to the reaction of ClO with NO_2, which becomes important as a result of the increasing HNO_3 photolysis rates when the air parcel moves southward. Although the gas phase formation of $ClONO_2$ is faster than that of HCl, the temperatures during nighttime during the warm period in the simulation are sufficiently low for heterogeneous hydrolysis of $ClONO_2$, whereas they are too high for heterogeneous conversion of HCl. Therefore the diurnal averaged rates of increase are comparable.

Figure 9 shows the fractions of the total active chlorine concentration (defined as Cl + ClO + $2Cl_2$ + $2Cl_2O_2$ + HOCl) to the total chlorine level, after adding (2), (3), and (4) successively. When the temperatures are close to 200 K, reactions (3) and (4), in combination with relatively low zenith angles, lead to significant production of active chlorine.

Figures 10a–10c show the temperature and pressure dependence of the γ values for (2)–(4). Increasing pressure and decreasing temperature cause a large increase of γ. Increasing ambient pressure results in increased water amounts in the aerosol due to the increase in relative humidity. The consequent decrease in sulfuric acid weight fraction leads to significant increase in the γ values of (2)–(4), as has been shown previously [*Hanson et al.*, 1994; *Hofmann and Oltmans*, 1992]. The sulfuric acid weight fraction (not shown) decreases from more than 70% for temperatures >210 K to 40% for temperatures <200 K and a pressure of 150 hPa. The increase of γ for (2) with pressure agrees with *Hofmann and Oltmans* [1992]. Figures 10a–10c also illustrate the importance for chlorine activation of the combination of low temperature and high pressure, as found in the trajectories used in this study. Note that the γ values at 200 K and 150 hPa are relatively high ($\geq 10^{-2}$ for (2) and (3) and 0.1 for (4)). *Hofmann and Oltmans* [1992] also discussed the combined effect of relatively high water vapor concentrations due to transport from the troposphere, and high pressure, which may be relevant for the lowermost stratosphere. Potential tropospheric influences have, however, not been taken into account here.

Figure 11 shows the timescales (τ) of heterogeneous conversion of HCl through (3) and (4) versus temperature at a pressure of 150 hPa. It can be seen that τ becomes smaller than 100 hours at temperatures below ~205 K for enhanced aerosol loading, and below ~200 K for background aerosol concentration, and increases to about 2 months in a relatively small temperature range. It is interesting to compare this lifetime with the number of hours that the air parcels are exposed to temperatures below 205 K. Figure 13 shows the maximum number of hours that the air parcels are continuously exposed to temperatures below ~200 K and below ~205 K. For temperatures below 205 K the average number of hours is 130, and 48 for temperatures below 200 K. Both exposure times are sufficient to cause significant chlorine activation, even if the air contained only background aerosol concentrations. Chlorine activation is further examined in Figure 12, which shows the temperature dependence of the Cl_2 production after 130 hours (solid lines) and 48 hours (dashed lines). There is significant Cl_2 production at 200 K after 50 hours and at 205 K after 130 hours for both enhanced and background aerosol abundance. This indicates that as the temperatures approach 200 K the production of active chlorine is more sensitive to temperature than to aerosol loading.

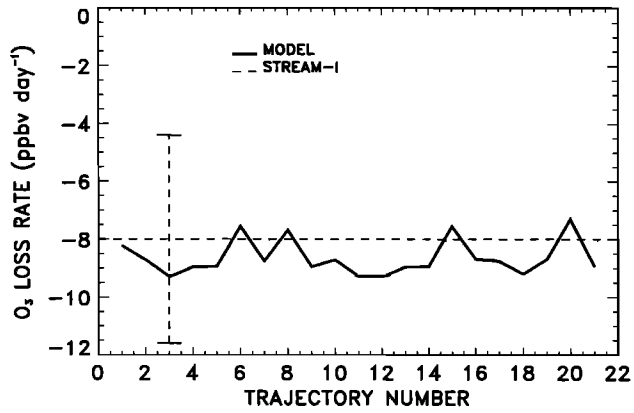

Figure 5. Calculated O_3 loss rates. The dashed lines represent the mean O_3 loss rate for the whole period considered, derived from the STREAM I observations. The uncertainty is indicated with the vertical line.

Figure 13 also shows the number of hours that the zenith angle was less than 90°, illustrating the small variation in sunlit hours between the different trajectories. The number of sunlit hours determines the ClO concentration and thus significantly affects O_3 loss, since ClO is the most important species in the O_3 loss cycles, as is illustrated in Figure 14a. Figures 14a and 14b show the contributions of the four most important O_3 loss cycles and the contributions of the heterogeneous reactions to O_3 loss. As expected, the ClO dimer cycle is the most important contributor to O_3 loss. Since HO_x concentrations are relatively low, the HO_x cycle is of minor importance, in contrast to middle-latitude conditions where ClO is relatively low [*Wennberg et al.*, 1994]. The reactions HO_2 + ClO and HO_2 + BrO (not shown) contribute even less to O_3 loss under these conditions. The contribution of the reaction BrO + ClO to the total O_3 loss is approximately 20%. The concentration of BrO is 100–1000 lower than ClO in the lower winter stratosphere [*Avallone et al.*, 1995; *Crewell et al.*, 1995; *Toohey et al.*, 1990; *Shindell et al.*, 1994]. The rate of the reaction BrO + ClO, however, is 2–3 orders of magnitude faster [*DeMore et al.*, 1994]. Hence this reaction contributes significantly to O_3 loss by 20–25% under background aerosol conditions, and 30% under enhanced aerosol conditions, which agrees with previous

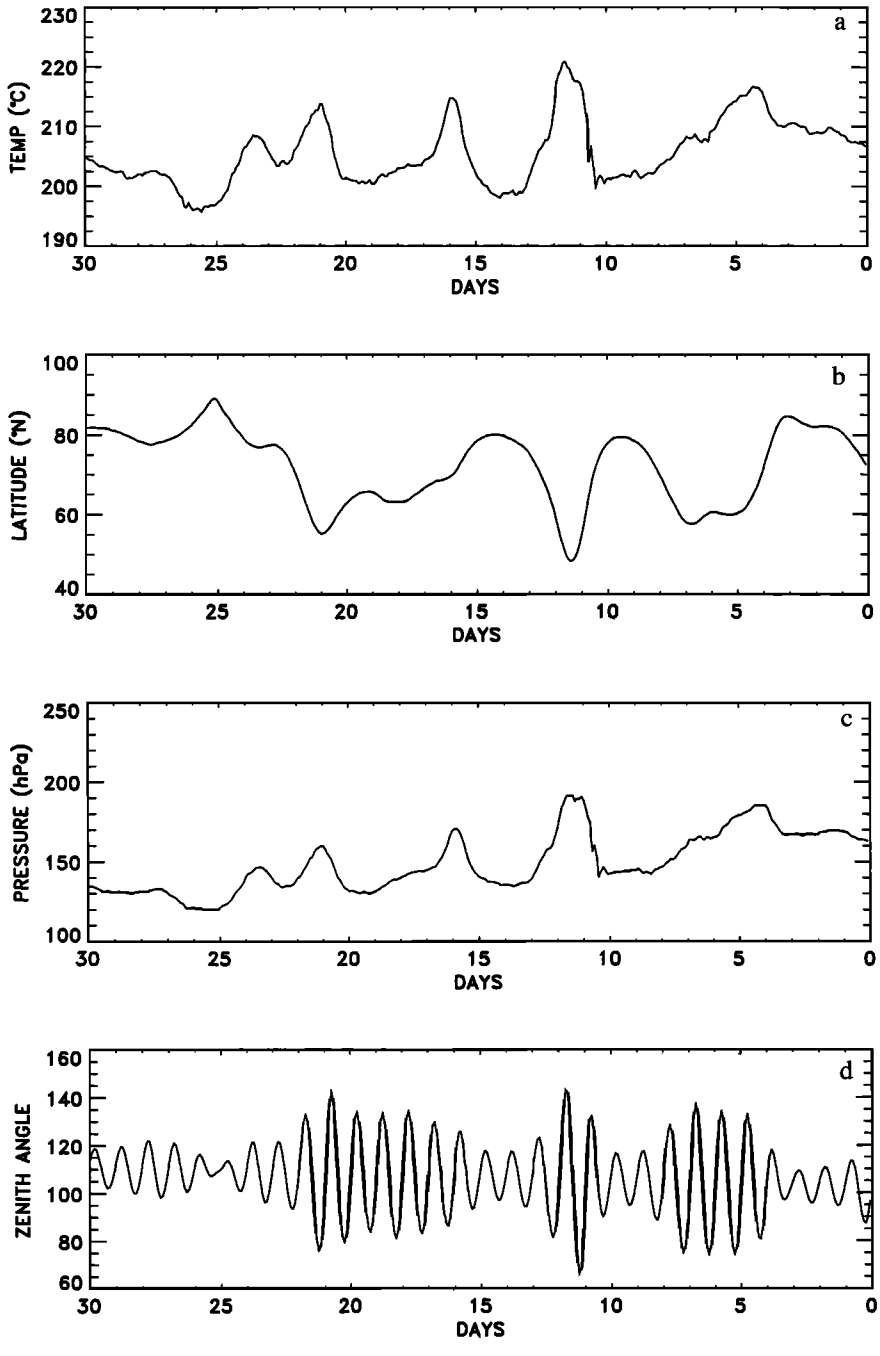

Figure 6. (a) Temperature (kelvins), (b) latitude, (c) pressure (hPa), and (d) zenith angle of trajectory 16.

model studies [*Anderson et al.*, 1989; *Solomon et al.*, 1990; *Danilin and McConnell*, 1995]. When no heterogeneous reactions are included, the O_3 loss rate is 3 ppbv d^{-1}, which is significantly lower than the observed O_3 loss rates. The contributions from both (3) and (4) to O_3 loss is significant, as can be seen in Figure 14b, and are needed to explain the observed O_3 loss rates. The calculated O_3 loss rates in Figures 14a and 14b show large variation from zero to more than 20 ppbv d^{-1}, corresponding to the variation of zenith angle and temperature, which significantly exceeds the averaged and observed loss rates. Therefore one should be cautious when using 10-day back trajectories to calculate O_3 loss, as they may not be representative for the whole O_3 destruction period.

Comparison With Model Results Using Back Trajectories on February 16 and 18

The back trajectories from February 16 and 18 are more variable and show relatively large excursions outside the vortex region [see *Bregman et al.*, 1995], implying that these air parcels are affected by mixing with air from midlatitudes. This is also indicated in Figure 1a by higher O_3 concentrations relative to N_2O for these air parcels. The temperatures of these trajectories are only occasionally below 210 K, so no significant chlorine activation occurred during the model simulation period. Consequently, the calculated O_3 concentrations after 30 days are close to the upper levels of the STREAM I estimates (see

Figure 9), which are about 100 ppbv higher compared to those using trajectory 16. This difference in O_3 concentration agrees with the observed O_3 loss rates multiplied by the estimated time difference that the air spent within the relatively cold vortex.

6. Sensitivity Analysis

Using trajectory 16 of February 17, which shows O_3 loss rates closest to the averaged loss rates, we performed a sensitivity analysis. Important parameters for O_3 loss, such as initial chlorine and bromine species, aerosol concentration, water vapor, HCl solubility, temperature, and zenith angle, were varied. The results are presented in Figure 15, showing the changes in O_3 loss rates (in parts per billion by volume per day) relative to the calculated overall mean O_3 loss rate.

Chlorine Species, BrO, and Water Vapor

Due to the importance of the ClO-dimer cycle on O_3 loss, it is clear that varying Cl_y concentrations will have a major effect on O_3 loss rates. Cl_y profiles from balloon measurements in the Arctic winter of 1992 [*Schmidt et al.*, 1994] and HF-Cl_y relations for February 1993 [*Müller et al.*, 1996] indicate Cl_y concentrations in the lowermost Arctic stratosphere of about 1000 pptv, which is 450 pptv lower than used in our simulations. This also agrees with Cl_y levels based on N_2O-Cl_y relations derived by [*Daniel et al.*, 1996]. Figure 15 shows that decreasing Cl_y by 450 pptv causes a decrease in calculated O_3 loss rates, which is significantly lower than the loss rates calculated by *Larsen et al.* [1994], but is still within the range derived from the STREAM data. Variation of the partitioning of different chlorine species within Cl_y was carried out by changing the ratio R = HCl/$ClONO_2$, and by initializing completely with active Cl (Cl_yres = 0%) and with chlorine reservoir species only (Cl_yres = 100%). Since HCl loss is faster than that of $ClONO_2$ under these conditions, increasing R results in an increase of O_3 loss rates and vice versa. However, the changes are relatively small (about 1 ppbv d^{-1}), even after changing initial Cl_yres from 0 to 100%, since both HCl and $ClONO_2$ are removed rapidly from the gas phase.

The calculated noon time BrO concentrations are about 2–3 pptv less than the mean concentrations at ER-2 altitudes (19–20 km altitude) [*Avallone et al.*, 1995]. Increasing the initial BrO concentration by a factor of 2 results in an increase of the O_3 loss rate by 1.5 ppbv d^{-1}. This change is about a factor of 2 less compared to changing Cl_y, because O_3 loss depends on the square of the ClO concentration, while it depends linearly on the BrO concentration.

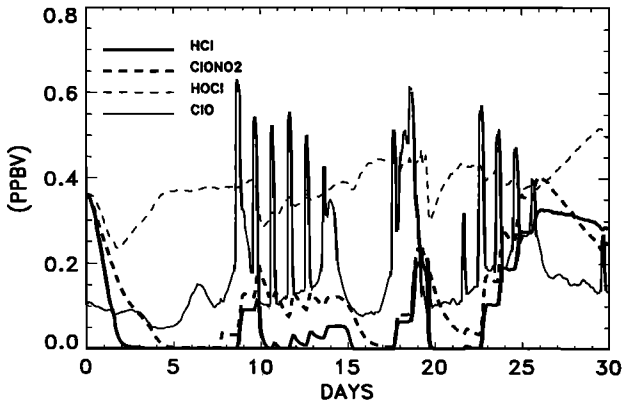

Figure 8. Model results (in parts per billion by volume) of HCl (thick solid line), $ClONO_2$ (thick dashed line), ClO (thin solid line), and HOCl (thin dashed line).

Increasing the water vapor concentration causes aerosol growth and dilution through increased condensation of the water molecules, and consequently a decrease of the sulfuric acid weight fraction. Since the uptake coefficients for (2)–(4) increase with decreasing sulfuric acid weight fraction, increasing the water vapor concentration causes enhanced chlorine activation and consequently enhanced O_3 loss. Increasing the water vapor concentrations by a factor of 2 resulted in an increase of the O_3 loss rate by 0.9 ppbv d^{-1}.

The solubility of HCl, expressed as the effective Henry's law constant (H^*), is uncertain within a factor of 3–4 [*Carslaw et al.*, 1995a]. However, changing H^* by a factor of 5 leads to a minor change in O_3 loss rates, due to the fact that HCl is already removed from the gas phase during periods with low temperatures (Figure 8).

Aerosol Concentration

The aerosol profiles measured during February 1993 indicate variations in aerosol surface area of 15–20 μm^2 cm^{-3} [*Deshler and Oltmans*, 1997]. The effects on the O_3 loss rates are not significant when the aerosol surface area (A) was

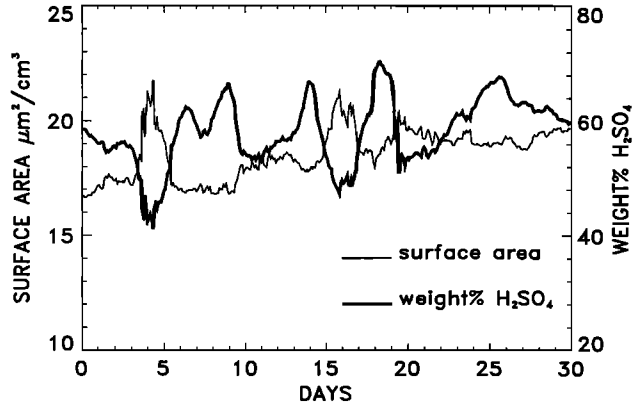

Figure 7. Calculated aerosol surface area (square micrometers per cubic centimeter) represented by the thin solid line, and sulfuric acid weight fraction (thick solid line).

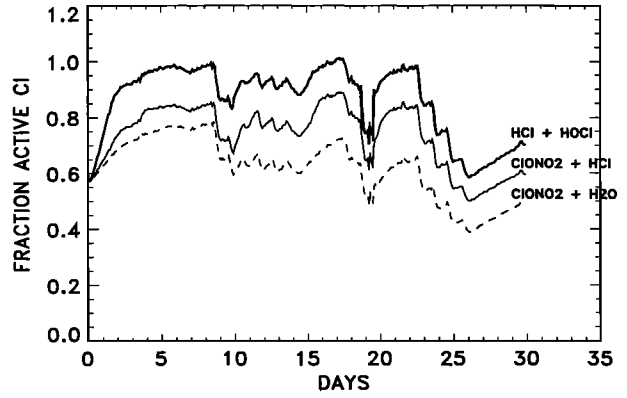

Figure 9. Model results of the fraction of active chlorine to the total chlorine level after including (1) to (4), successively (see text for details).

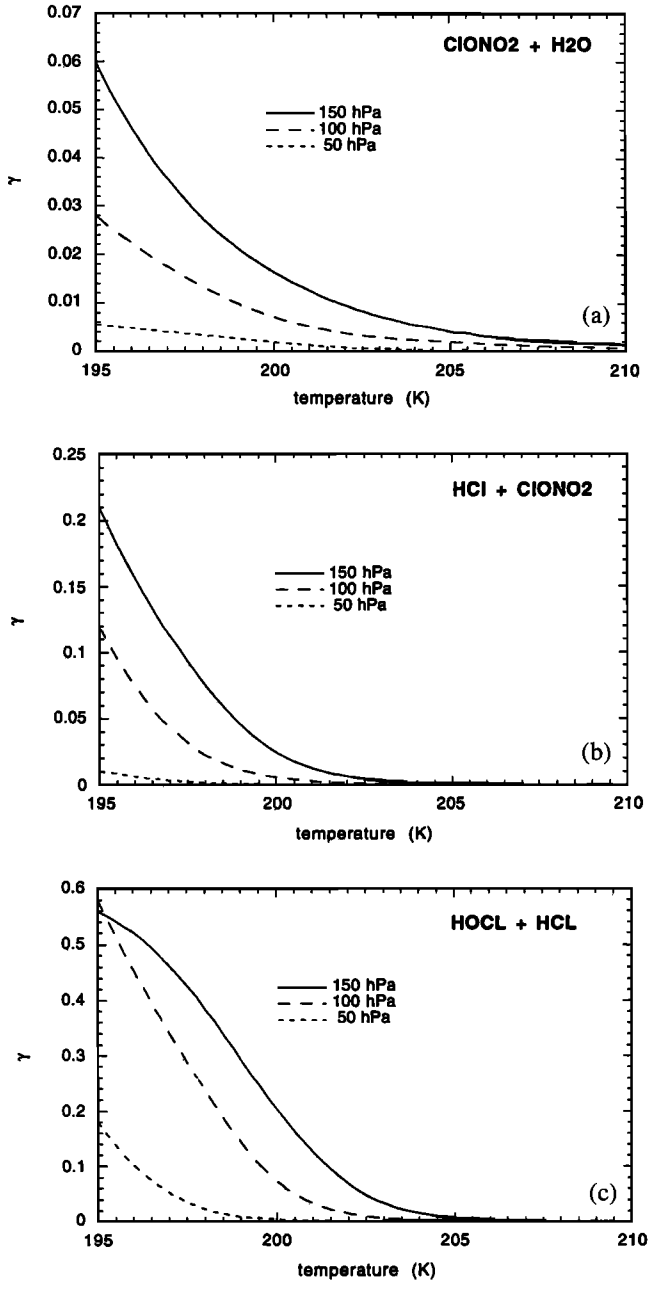

Figure 10. Dependence of the uptake coefficient for (2)–(4) on temperature and pressure.

increased by a factor of 2. This may be expected, since the N_2O_5, $ClONO_2$, and HCl concentrations are reduced after relatively fast heterogeneous removal during periods of enhanced aerosol loading, so further increases of A do not lead to increased removal of chlorine reservoir species. Decreasing the aerosol concentration to background levels (A = 1 μm^2 cm^{-3}) causes a decrease in O_3 loss rates, although the decrease is relatively small, as was illustrated earlier. This will be discussed further in section 7. Further experiments were performed by allowing NAT formation at the NAT equilibrium temperature. The presence of NAT did not, however, result in higher O_3 loss rates (not shown). This is because nearly complete conversion of chlorine reservoir species to active chlorine species already occurred using liquid aerosols, as is discussed later.

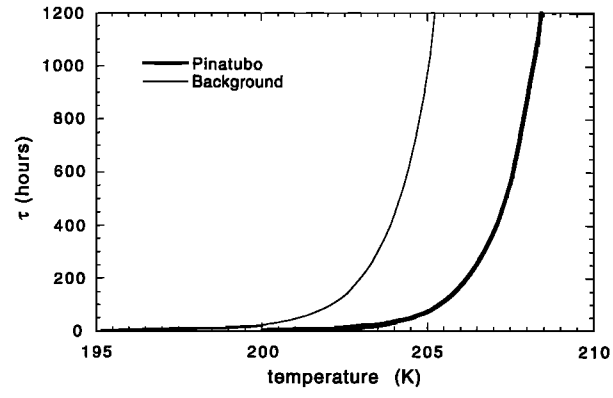

Figure 11. The timescale of heterogeneous conversion of HCl by (3) and (4) versus temperature with background and enhanced aerosol concentrations.

Trajectory Temperature and Zenith Angle

Potential sources of uncertainty are the back trajectory temperature and latitudes. Lower temperatures and lower latitudes (thus smaller zenith angles) accelerate chlorine activation. A comparison between temperatures from the ECMWF analyses at 30 hPa at high latitudes in January 1992 and radiosondes reveals an overestimation in the ECMWF analyses of approximately 5 K [*Naujokat*, 1994]. In addition, *Knudsen et al.* [1996] compared ECMWF temperatures with balloon measurements and found that the ECWMF temperatures inside the vortex at 50 hPa for January 1993 were 1–5 K higher. However, they also show a decrease in temperature deviation with increasing pressure; at 70 hPa the deviation was only 0–2 K for the balloon flights in January 1993. Decreasing the trajectory temperature by 5 K in our calculations caused an increase in O_3 loss rates of 1.3 ppbv d^{-1}. The uncertainty in the trajectory locations is difficult to estimate. We changed all trajectory latitudes by 2.5° southward and northward, so that the zenith angles decreased and increased, respectively, leading to an increase of O_3 loss rates of 1.5 ppbv d^{-1} and a decrease of 2 ppbv d^{-1}.

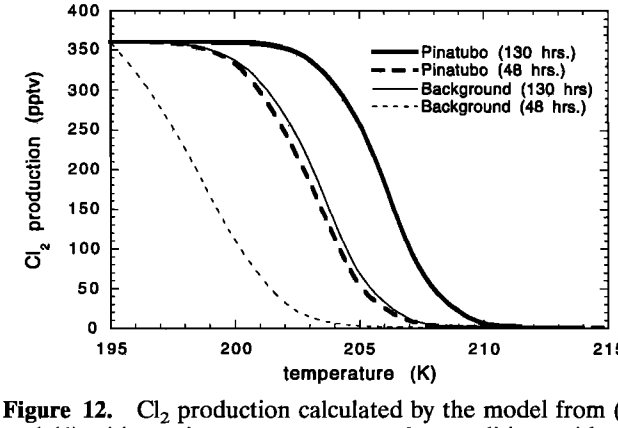

Figure 12. Cl_2 production calculated by the model from (3) and (4) with varying temperatures under conditions with enhanced aerosol loading (thick lines) and background aerosol levels (thin lines).

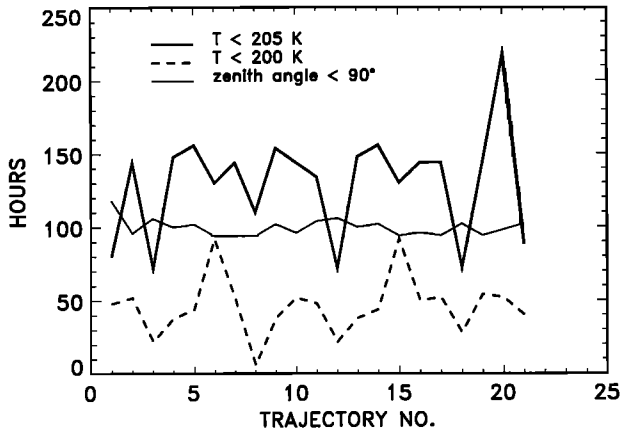

Figure 13. Maximum number of hours that the trajectory air parcels are continuously exposed to temperatures ≤205 K (thick solid line), and ≤200 K (thick dashed line). The thin solid line shows the number of hours that the zenith angle was lower than 90°.

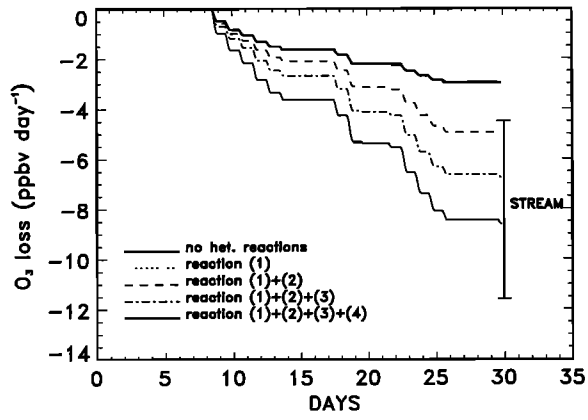

Figure 14b. Model results of the fractional contribution to total O_3 loss from a simulation without heterogeneous reactions and heterogeneous reactions (1) to (4) (see text for details). The vertical line represents the range of the observed O_3 loss rates from the STREAM I data.

7. Discussion and Conclusions

A chemistry-trajectory model was used to calculate O_3 loss rates in the lowermost Arctic winter stratosphere during January and February 1993. The calculated O_3 loss rate was 8.6 ppbv (1.3% d^{-1}), in good agreement with estimations from observations for the same period.

The level of Cl_y has a significant effect on O_3 loss rates due to the importance of the ClO dimer cycle. The simulations with Cl_y levels as obtained from in situ measurements [*Woodbridge et al.*, 1995] show nearly complete chlorine activation, consistent with observations. The noon values of ClO, however, do not agree with measurements performed in the Arctic polar vortex in February 1993 [*Crewell et al.*, 1995; *Shindell et al.*, 1994]. Their results indicate ClO concentrations between 100 and 300 pptv inside the vortex below 125 hPa, whereas the calculated noon ClO mixing ratios are 1.5 times higher at 75°N and 2 times higher at 65°N (Figure 8). Using Cl_y mixing ratios of 1000 pptv obtained from other N_2O-Cl_y relations [*Daniel et al.*, 1996] and from balloon measurements [*Schmidt et al.*, 1994] results in calculated O_3 loss rates that are about 3 ppbv d^{-1} lower. These loss rates are at the lower edge but still within the observed range derived from the STREAM I data. However, the range is large and there are no observed O_3 loss rates derived from other data at potential temperature levels below 380 K.

The use of 30-day back trajectories introduces errors in the simulated temperatures and latitudes of the air parcels (and thus the zenith angle). Sensitivity analysis reveals that an decrease in the trajectory temperatures by 5 K causes an increase in O_3 loss rates to 9.9 ppbv d^{-1}. A change of the latitudes by 2.5° causes a change in O_3 loss rates to 6.6–10.1 ppbv d^{-1}. This also indicates that O_3 loss rate calculations are sensitive to the period, i.e., the trajectory lengths considered, as is illustrated in Figures 14a and 14b. However, there is no evidence of systematic underprediction or overprediction of latitude from the trajectory computations. Moreover, it is expected that at relatively high pressure levels the temperatures may not or only slightly be overpredicted by the ECMWF [*Knudsen et al.*, 1996]. Further, errors in the calculation of the wind perpendicular to the isotherms (v) would imply uncertainties in the trajectory temperatures and the cooling rates and thus in the O_3 loss rates. But a change of v of only 1 m s^{-1} induces a change in $d\theta/dt$ of 1.5 K d^{-1} (P. Siegmund, personal communication, 1996), which is significantly larger than the 1-σ values found from $d\theta/dt$ of all 21 trajectories.

Heterogeneous reactions on liquid sulfuric acid aerosols involving $ClONO_2$ and HCl must be considered in the model to explain the observed O_3 loss rates. Changing the aerosol load-

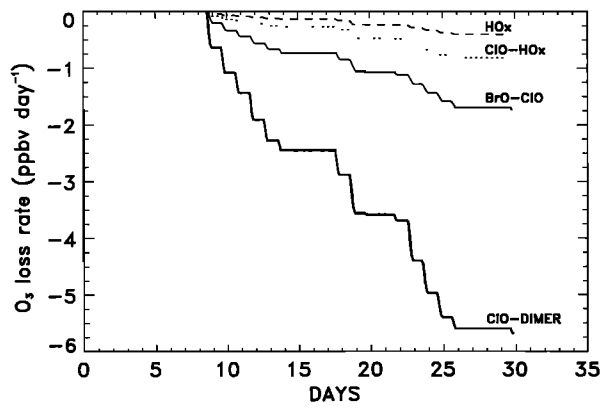

Figure 14a. Model results of the fractional contribution to total O_3 loss from the four major O_3 depletion cycles.

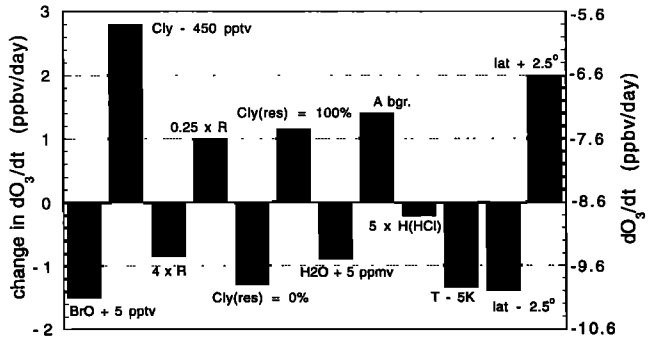

Figure 15. Sensitivity of calculated O_3 loss rates (parts per billion by volume per day) to changes in different variables relevant for O_3 loss.

ing to background levels has a relatively small effect on O_3 loss rates. The temperatures are sufficiently low to cause significant chlorine activation, even if the air had contained only background aerosol concentrations. Figure 12 illustrates that for the conditions during January-February 1993 in the lowermost Arctic stratosphere, at temperatures $\leq$200 K, there is no difference in Cl_2 production between conditions with background and enhanced aerosol levels. This implies that O_3 loss is more sensitive to temperature changes than to changes in aerosol concentrations when the temperatures are sufficiently low for significant chlorine activation. The observed negative temperature trend in the lower stratosphere [*Oort and Liu*, 1993; *Angell*, 1988] may thus have contributed to the observed negative O_3 trends by increased O_3 loss, even under background aerosol levels. It is also important to stress that the vortex edge at 160 hPa was occasionally located at middle latitudes. "Vortex O_3 chemistry" may therefore contribute to the negative O_3 trends at middle latitudes under meteorological conditions which favor a well-developed vortex at relatively low altitudes.

Appendix

A linear least squares method is applied to calculate the O_3 loss rates from the STREAM I observations. The solid lines in Figures 1a and 1b represent the fitting vectors containing the dependent coordinates O_3 and θ. The differences of the dependent coordinates can be calculated for each N_2O concentration.

Since the equations are assumed linear with the form

$$Y = \alpha X + D$$

with $Y = O_3$ or θ, and $X = N_2O$, ΔY is the difference in O_3 or θ levels between the relations of February 17 and February 16 and 18 for a constant N_2O concentration. The precision of the differences, δY, is calculated from the 1-σ values of $Y(\sigma_y)$:

$$\Delta Z = Z\sqrt{\left(\frac{\sigma_y(1)}{\Delta Y(1)}\right)^2 + \left(\frac{\sigma_y(2)}{\Delta Y(2)}\right)^2} \quad (5)$$

The indices 1 and 2 correspond to the two relations in the figures.

The cooling rate $d\theta/dt$ and ΔY (with $Y = \theta$) can be used to estimate the time difference, Δ days. The precision, δ days, is calculated with

$$\delta Z = Z\sqrt{\left(\frac{\delta X}{\Delta X}\right)^2 + \left(\frac{\delta Y}{\Delta Y}\right)^2} \quad (6)$$

with $Z = \Delta$ days, $X = d\theta/dt$, and $Y = \Delta\theta$.

The O_3 loss rate, dO_3/dt, can then be calculated from ΔO_3 and Δ days, and the precision is obtained from (6) with $Z = dO_3/dt$, $X = \Delta O_3$, and $Y = \Delta$ days.

An example is given for N_2O = 240 ppbv. Based on the fitting equations: $\Delta O_3(240)$ = 122 ppbv and $\Delta\theta(240)$ = 8.8 K, the 1-σ values are $\sigma O_3(1)$ = 18.68 ppbv, $\sigma O_3(2)$ = 23.89 ppbv, $\sigma\theta(1)$ = 1.83 K, and $\sigma\theta(2)$ = 2.69 K.

$$\frac{d\theta}{dt} \pm \delta\left(\frac{d\theta}{dt}\right) = -0.6 \pm 0.06 \text{ K}$$

[*Larsen et al.*, 1994]; hence Δ days $\pm$ δ days = 14.7 $\pm$ 5.6 days and

$$\frac{dO_3}{dt} \pm \delta\left(\frac{dO_3}{dt}\right) = 8.0 \pm 3.6 \text{ ppbv d}^{-1}.$$

Acknowledgments. This work was supported by the Netherlands Organization for Scientific Research (NWO) in the framework of the National Research Program (NOP) for Global Pollution and Climate Change. The STREAM project is supported by the European Commission. The N_2O data were kindly provided by the Max Planck Institute for Chemistry in Mainz (Horst Fischer, Frank Wienhold, and Thomas Zenker), and the O_3 data by the University of Wageningen (Michel Bolder). The authors thank David Lary for making available his radiative transfer code and Peter Siegmund and Peter van Velthoven for helpful comments and meteorological support. We further acknowledge useful comments from an anonymous reviewer.

References

Anderson, J. G., et al., Kinetics of O_3 destruction by ClO and BrO within the Antarctic vortex: An analysis based on in situ ER-2 data, *J. Geophys. Res.*, *94*, 11,480–11,520, 1989.

Angell, J. K., Variations and trends in tropospheric and stratospheric global temperatures, 1958–1987, *J. Clim.*, *1*, 1296–1313, 1988.

Austin, J., N. Butchart, and K. P. Shine, Possibility of an Arctic ozone hole in a doubled-CO_2 climate, *Nature*, *360*, 221–225, 1994.

Avallone, L. M., et al., In situ measurements of BrO during AASE II, *Geophys. Res. Lett.*, *22*, 831–834, 1995.

Blom, C. E., H. Fischer, N. Glatthor, T. Gulde, M. Höpfner, and C. Piesch, Spatial and temporal variability of $ClONO_2$, HNO_3, and O_3 in the Arctic winter of 1992/1993 as obtained by airborne infrared emission spectroscopy, *J. Geophys. Res.*, *100*, 9101–9114, 1995.

Bojkov, R. D., et al., Record low total ozone during northern winters of 1992 and 1993, *Geophys. Res. Lett.*, *20*, 1351–1354, 1993.

Braathen, G. O., et al., Temporal development of ozone within the Arctic vortex during the winter of 1991/1992, *Geophys. Res. Lett.*, *21*, 1407–1410, 1994.

Brasseur, G., and C. Granier, Mount Pinatubo aerosols, chlorofluorcarbons, and ozone depletion, *Science*, *257*, 1239–1241, 1992.

Brasseur, G., and S. Solomon, *Aeronomy of the Middle Atmosphere*, 2nd ed., D. Reidel, Norwell, Mass., 1986.

Bregman, A., et al., Aircraft measurements of O_3, HNO_3, and N_2O in the winter Arctic lower stratosphere during the Stratosphere-Troposphere Experiment by Aircraft Measurements (STREAM) I, *J. Geophys. Res.*, *100*, 11,245–11,260, 1995.

Browell, E. V., et al., Ozone and aerosol changes during the 1991–1992 Airborne Arctic Stratospheric Expedition, *Science*, *261*, 1155–1158, 1993.

Brühl, C., and P. J. Crutzen, MPIC two-dimensional model, in The Atmospheric Effect of Stratospheric Aircraft, edited by M. J. Prather and E. E. Remsberg, *NASA Ref. Publ.*, *1292*, 103–104, 1993.

Burkholder, J. B., R. K. Talukdar, A. R. Ravishankara, and S. Solomon, Temperature dependence of the HNO_3 UV absorption cross sections, *J. Geophys. Res.*, *98*, 22,937–22,948, 1993.

Carslaw, K. S., The properties of aqueous stratospheric aerosols and the depletion of ozone, Ph.D. thesis, Univ. of East Anglia, Norwich, England, 1994.

Carslaw, K. S., B. P. Luo, S. L. Clegg, T. Peter, P. Brimblecombe, and P. J. Crutzen, Stratospheric aerosol growth and HNO_3 gas phase depletion from coupled HNO_3 and water uptake by liquid particles, *Geophys. Res. Lett.*, *21*, 2479–2482, 1994.

Carslaw, K. S., S. L. Clegg, and P. Brimblecombe, A thermodynamic model of the HCl-HNO_3-H_2SO_4-H_2O, including solubilities of HBr, from <200 K to 328 K, *J. Phys. Chem.*, *99*, 11,557–11,574, 1995a.

Carslaw, K. S., B. Luo, and T. Peter, An analytical expression for the composition of aqueous HNO_3-H_2SO_4 stratospheric aerosols including gas phase removal of HNO_3, *Geophys. Res. Lett.*, *22*, 1877–1880, 1995b.

Chipperfield, M. P., et al., The variability of $ClONO_2$ and HNO_3 in the Arctic polar vortex: Comparison of Transall Michelsen interferometer for passive atmospheric sounding measurements and three-dimensional model results, *J. Geophys. Res.*, *100*, 9115–9129, 1995.

Collins, J. E., G. W. Sasche, B. E. Anderson, A. J. Weinheimer, J. G. Walega, and B. A. Ridley, AASE-II in-situ tracer correlations of methane, nitrous oxide, and ozone as observed aboard the DC-8, *Geophys. Res. Lett.*, *20*, 2543–2546, 1993.

Crewell, S., R. Fabian, K. Künzi, and T. Wehr, Comparison of ClO measurements by airborne and spaceborne microwave radiometers in the Arctic winter stratosphere 1993, *Geophys. Res. Lett.*, *22*, 1489–1492, 1995.

Crutzen, P. J., R. Müller, C. Brühl, and T. Peter, On the potential

importance of the gas phase reaction $CH_3O_2 + ClO \rightarrow ClOO + CH_3O$ and the heterogeneous reaction $HOCl + HCl \rightarrow H_2O + Cl_2$ in "ozone hole" chemistry, *Geophys. Res. Lett.*, *19*, 1113–1116, 1992.

Dahlberg, S. P., and K. P. Bowman, Isentropic mixing in the Arctic stratosphere during the 1992–1993 and 1993–1994 winters, *Geophys. Res. Lett.*, *22*, 1237–1240, 1995.

Daniel, J. S., et al., On the age of stratospheric air and inorganic chlorine and bromine release, *J. Geophys. Res.*, *101*, 16,757–16,770, 1996.

Danilin, M. Y., and J. C. McConnell, Stratospheric effects of bromine activation on/in sulfate aerosol, *J. Geophys. Res.*, *100*, 11,237–11,243, 1995.

DeMore, W. B., et al., Chemical kinetics and photochemical data for use in stratospheric modelling: Evaluation number 11, *JPL Publ. 94-26*, Jet Propul. Lab., Pasadena, Calif., 1994.

Deshler, T., and S. J. Oltmans, Vertical profiles of volcanic aerosol and polar stratospheric clouds above Kiruna Sweden, winters 1993 and 1995, *J. Atmos. Chem.*, in press, 1997.

Deshler, T., B. J. Johnson, and W. R. Rozier, Balloonborne measurements of Pinatubo aerosol during 1991 and 1992 at 41°N: Vertical profiles, size distributions, and volatility, *Geophys. Res. Lett.*, *20*, 1435–1438, 1993.

Drdla, K., A. Tabazadeh, R. P. Turco, and M. Z. Jacobson, Analysis of the physical state of one Arctic polar stratospheric cloud based on observations, *Geophys. Res. Lett.*, *21*, 2475–2478, 1994.

Fabian, P., R. Borchers, and K. Kourtidis, Bromine-containing source gases during EASOE, *Geophys. Res. Lett.*, *21*, 1219–1222, 1994.

Fried, A., B. A. Henry, J. G. Calvert, and M. Mozurkewich, The reaction probability of N_2O_5 with sulfuric acid aerosols at stratospheric temperatures and compositions, *J. Geophys. Res.*, *99*, 3517–3532, 1994.

Granier, C., and G. Brasseur, Impact of heterogeneous chemistry on model predictions of ozone changes, *J. Geophys. Res.*, *97*, 18,015–18,033, 1992.

Hanson, D. R., and E. R. Lovejoy, The uptake of N_2O_5 onto small sulfuric acid particles, *Geophys. Res. Lett.*, *21*, 2401–2404, 1994.

Hanson, D. R., and K. Mauersberger, Vapor pressures of HNO_3/H_2O solutions at low temperatures, *J. Phys. Chem.*, *92*, 6167–6170, 1988.

Hanson, D. R., and A. R. Ravishankara, Uptake of HCl and HOCl onto sulfuric acid: Solubilities, diffusivities, and reaction, *J. Phys. Chem.*, *97*, 12,309–12,319, 1993.

Hanson, D. R., and A. R. Ravishankara, Reactive uptake of $ClONO_2$ onto sulfuric acid due to reaction with HCl and H_2O, *J. Phys. Chem.*, *98*, 5728–5735, 1994.

Hanson, D. R., A. R. Ravishankara, and S. Solomon, Heterogeneous reactions in sulfuric acid aerosols: A framework for model calculations, *J. Geophys. Res.*, *99*, 3617–3629, 1994.

Hofmann, D. J., and S. J. Oltmans, The effect of stratospheric water vapor on the heterogeneous reaction rate of $ClONO_2$ and H_2O for sulfuric acid aerosol, *Geophys. Res. Lett.*, *19*, 2211–2214, 1992.

Huthwelker, T., T. Peter, B. P. Luo, S. L. Clegg, K. S. Carslaw, and P. Brimblecombe, Solubility of HOCl in water and aqueous H_2SO_4 to stratospheric temperatures, *J. Atmos. Chem.*, *21*, 81–95, 1995.

Johnson, D. G., W. A. Traub, K. V. Chance, and K. W. Jucks, Detection of HBr and upper limit for HOBr: Bromine partitioning in the stratosphere, *Geophys. Res. Lett.*, *22*, 1373–1376, 1995.

Jones, R. L., and A. R. MacKenzie, Observational studies of the role of polar regions in midlatitude ozone loss, *Geophys. Res. Lett.*, *22*, 3485–3488, 1995.

Kawa, S. R., D. W. Fahey, L. E. Heidt, W. H. Pollock, S. Solomon, D. E. Anderson, M. Loewenstein, M. H. Proffitt, J. J. Margitan, and K. R. Chan, Photochemical partitioning of the reactive nitrogen and chlorine reservoirs in the high-latitude stratosphere, *J. Geophys. Res.*, *97*, 7905–7923, 1992.

Kerr, J. B., D. I. Wardle, and D. W. Tarasick, Record low ozone values over Canada in early 1993, *Geophys. Res. Lett.*, *20*, 1979–1982, 1993.

Knudsen, B. M., J. M. Rosen, N. T. Kjome, and A. T. Whitten, Comparison of analyzed stratospheric temperatures and calculated trajectories with long-duration balloon data, *J. Geophys. Res.*, *101*, 19,137–19,145, 1996.

Komhyr, W. D., et al., Unprecedented 1993 ozone decrease over the United States from Dobson spectrometer observations, *Geophys. Res. Lett.*, *21*, 201–204, 1994.

Larsen, N., et al., Ozone depletion in the Arctic stratosphere in early 1993, *Geophys. Res. Lett.*, *21*, 1611–1614, 1994.

Lary, D. J., and J. A. Pyle, Diffuse radiation, twilight and photochemistry, *J. Atmos. Chem.*, *13*, 373–406, 1991.

Lefèvre, F., et al., Chemistry of the 1991–1992 stratospheric winter: Three-dimensional model simulations, *J. Geophys. Res.*, *99*, 8183–8195, 1994.

Luo, B., S. L. Clegg, T. Peter, R. Müller, and P. J. Crutzen, HCl solubility and liquid diffusion in aqueous sulfuric acid under stratospheric conditions, *Geophys. Res. Lett.*, *21*, 49–52, 1994.

Luo, B., K. S. Carslaw, T. Peter, and S. L. Clegg, Vapor pressures of $H_2SO_4/HNO_3/HCl/HBr/H_2O$ solutions to low stratospheric temperatures, *Geophys. Res. Lett.*, *22*, 247–250, 1995.

Manney, G. L., R. W. Zurek, M. E. Gelman, A. J. Miller, and R. Nagatani, The anomalous Arctic lower stratospheric polar vortex of 1992–1993, *Geophys. Res. Lett.*, *21*, 2405–2408, 1994a.

Manney, G. L., R. W. Zurek, A. O'Neill, and R. Swinbank, On the motion of air through the stratospheric polar vortex, *J. Atmos. Sci.*, *51*, 2973–2994, 1994b.

Manney, G. L., et al., Chemical depletion of ozone in the Arctic lower stratosphere during winter 1992–1993, *Nature*, *370*, 429–433, 1994c.

Manney, G. L., L. Froidevaux, J. W. Waters, and R. W. Zurek, Evolution of microwave limbsounder ozone and the polar vortex during winter, *J. Geophys. Res.*, *100*, 2953–2972, 1995.

McKenna, D. S., et al., Calculations of ozone destruction during the 1988/89 Arctic winter, *Geophys. Res. Lett.*, *17*, 553–556, 1990.

Michelsen, H. A., R. J. Salawitch, P. O. Wennberg, and J. G. Anderson, Production of $O(^1D)$ from photolysis of O_3, *Geophys. Res. Lett.*, *21*, 2227–2230, 1994.

Müller, R., and P. J. Crutzen, Chlorine activation mechanisms during the polar night, *J. Geophys. Res.*, *98*, 20,483–20,490, 1993.

Müller, R., et al., Chlorine chemistry and the potential for ozone depletion in the Arctic stratosphere in the winter of 1991/92, *Geophys. Res. Lett.*, *21*, 1427–1430, 1994.

Müller, R., P. J. Crutzen, J.-U. Grooss, C. Brühl, J. M. Russell III, and A. F. Tuck, Chlorine activation and ozone depletion in the Arctic vortex: Observations by the Halogen Occultation Experiment on the Upper Atmospheric Research Satellite, *J. Geophys. Res.*, *101*, 12,531–12,554, 1996.

National Oceanic and Atmospheric Administration (NOAA), Northern hemisphere winter summary, 1992–1993, in *NOAA Climate Analysis Center Report*, Silver Spring, Md., April 15, 1993.

Naujokat, B., A synoptic view of the ECMWF stratospheric forecasts, in *Proceedings, Stratosphere and Numerical Weather Prediction*, Eur. Cent. for Medium Range Weather Forecasts, Reading, England, 1994.

Notholt, J., P. von der Gathen, and S. Peil, Heterogeneous conversion of HCl and $ClONO_2$ during the Arctic winter 1992/1993 initiating ozone depletion, *J. Geophys. Res.*, *100*, 11,269–11,274, 1995.

Oort, A. H., and H. Liu, Upper air temperature trends over the globe, 1958–1989, *J. Clim.*, *6*, 292–307, 1993.

Pitari, G., and V. Rizi, An estimate of the chemical and radiative perturbation of stratospheric ozone following the eruption of Mt. Pinatubo, *J. Atmos. Sci.*, *50*, 3260–3276, 1993.

Plumb, R. A., and M. K. W. Ko, Interrelationships between mixing ratios of long-lived stratospheric constituents, *J. Geophys. Res.*, *97*, 10,145–10,156, 1992.

Poole, L. R., and M. C. Pitts, Polar stratospheric cloud climatology based on Stratospheric Aerosol Measurement II observations from 1978 to 1989, *J. Geophys. Res.*, *99*, 13,083–13,089, 1994.

Proffitt, M. H., J. J. Margitan, K. K. Kelly, M. Loewenstein, J. R. Podolske, and K. R. Chan, Ozone loss in the Arctic polar vortex inferred from high-altitude aircraft, *Nature*, *347*, 31–36, 1990.

Proffitt, M. H., et al., Ozone loss inside the northern polar vortex during the 1991–1992 winter, *Science*, *261*, 1150–1154, 1993.

Pueschel, R. F., P. B. Russell, D. A. Allen, G. V. Ferry, and K. G. Snetsinger, Physical and optical properties of the Pinatubo volcanic aerosol: Aircraft observations with impactors and a Sun-tracking photometer, *J. Geophys. Res.*, *99*, 12,915–12,922, 1994.

Randel, W. J., F. Wu, J. M. Russell III, J. W. Waters, and L. Froidevaux, Ozone and temperature changes in the stratosphere following the eruption of Mount Pinatubo, *J. Geophys. Res.*, *100*, 16,753–16,764, 1995.

Roche, A. E., et al., Observations of lower stratospheric $ClONO_2$, HNO_3, and aerosol by the UARS CLAES Experiment between January 1992 and April 1993, *J. Atmos. Sci.*, *51*, 2877–2902, 1994.

Rodriguez, J. M., M. K. W. Ko, and N. D. Sze, Role of heterogeneous

conversion of N_2O_5 on sulfate aerosols in global ozone losses, *Nature*, *352*, 134–137, 1991.

Rodriguez, J. M., et al., Ozone response to enhanced heterogeneous processing after the eruption of Mt. Pinatubo, *Geophys. Res. Lett.*, *21*, 209–212, 1994.

Rosen, J. M., N. T. Kjome, and S. J. Oltmans, Simultaneous ozone and polar stratospheric cloud observations at south pole during winter and spring 1991, *J. Geophys. Res.*, *98*, 12,741–12,751, 1993.

Rosen, J. M., N. T. Kjome, H. Fast, and N. Larsen, Volcanic aerosol and polar stratospheric clouds in the winter 1992/93 north polar vortex, *Geophys. Res. Lett.*, *21*, 61–64, 1994.

Schmidt, U., R. Bauer, A. Engel, R. Borchers, and J. Lee, The variation of available chlorine, Cl_y, in the Arctic polar vortex during EASOE, *Geophys. Res. Lett.*, *21*, 1215–1218, 1994.

Schoeberl, M. R., L. R. Lait, P. A. Newman, and J. E. Rosenfield, The structure of the polar vortex, *J. Geophys. Res.*, *97*, 7859–7882, 1992.

Shindell, D. T., J. M. Reeves, L. K. Emmons, and R. L. de Zafra, Arctic chlorine monoxide observations during spring 1993 over Thule, Greenland, and implications for ozone depletion, *J. Geophys. Res.*, *99*, 25,697–25,704, 1994.

Solomon, S., et al., Progress towards a quantitative understanding of Antarctic ozone depletion, *Nature*, *347*, 347–354, 1990.

Stone, R. S., J. R. Key, and E. G. Dutton, Properties and decay of stratospheric aerosols in the Arctic following the 1991 eruptions of Mount Pinatubo, *Geophys. Res. Lett.*, *20*, 2359–2362, 1993.

Tabazadeh, A., et al., A study of type I polar stratospheric cloud formation, *Geophys. Res. Lett.*, *21*, 1619–1621, 1994.

Tie, X., G. P. Brasseur, B. Briegleb, and C. Granier, Two-dimensional simulation of Pinatubo aerosol and its effect on stratospheric ozone, *J. Geophys. Res.*, *99*, 20,545–20,562, 1994.

Toohey, D. W., et al., In situ measurements of BrO in the Arctic stratosphere, *Geophys. Res. Lett.*, *17*, 513–516, 1990.

Toohey, D. W., et al., The seasonal evolution of reactive chlorine in the northern hemisphere stratosphere, *Science*, *261*, 1134–1136, 1993.

Trepte, C. R., R. E. Veiga, and M. P. McCormick, The poleward dispersal of Mount Pinatubo volcanic aerosol, *J. Geophys. Res.*, *98*, 18,563–18,573, 1993.

Turco, R. P., et al., Physicochemistry of the polar ozone hole, *J. Geophys. Res.*, *94*, 16,493–16,510, 1989.

von Clarmann, T., H. Fischer, F. Friedl-Vallon, A. Linden, H. Oelhaf, C. Piesch, M. Seefeldner, and W. Völker, Retrieval of stratospheric O_3, HNO_3, and $ClONO_2$ profiles from 1992 MIPAS-B limb emission spectra: Method, result and error analysis, *J. Geophys. Res.*, *98*, 20,495–20,506, 1993.

von Clarmann, T., A. Linden, H. Oelhaf, H. Fischer, F. Friedl-Vallon, C. Piesch, and M. Seefeldner, Determination of the stratospheric organic chlorine budget in the spring Arctic vortex from MIPAS-B limb emission spectra and air sampling experiments, *J. Geophys. Res.*, *100*, 13,979–13,997, 1995.

Waters, J. W., et al., Stratospheric ClO and ozone from the microwave limb sounder on the Upper Atmospheric Research Satellite, *Science*, *362*, 597–602, 1993.

Waters, J. W., G. J. Manney, W. G. Read, L. Froidevaux, D. A. Flower, and R. F. Jarnot, UARS MLS observations of lower stratospheric ClO in the 1992–1993 and 1993–1994 Arctic winter vortex, *Geophys. Res. Lett.*, *22*, 823–826, 1995.

Webster, C. R., et al., Chlorine chemistry on polar stratospheric cloud particles in the Arctic winter, *Science*, *261*, 1130–1134, 1993.

Wennberg, P. O., et al., Removal of stratospheric O_3 by radicals: In situ measurements of OH, HO_2, NO, NO_2, ClO, and BrO, *Science*, *266*, 398–404, 1994.

Woodbridge, E. L., et al., Estimates of total organic and inorganic chlorine in the lower stratosphere from in situ and flask measurements during AASE II, *J. Geophys. Res.*, *100*, 3057–3064, 1995.

World Meteorological Organization (WMO), Scientific assessment of O_3 depletion: 1994, *Rep. 37*, Geneva, 1994.

A. Bregman and J. Lelieveld, Institute for Marine and Atmospheric Research Utrecht, Princetonplein 5, 3584 CC Utrecht, Netherlands. (e-mail: bregman@fys.ruu.nl; mvdbroek@fys.ruu.nl; lelievld@fys.ruu.nl)

M. M. P. van den Broek, Space Research Organisation of the Netherlands, Sorbonnelaan 2, 3584 CA Utrecht, Netherlands.

K. S. Carslaw and T. Peter, Max Planck Institute for Chemistry, Aerosol Group, P. O. Box 3060, D-55020 Mainz, Germany. (e-mail: carslaw@nike.mpch-mainz.mpg.de; peter@nike.mpch-mainz.mpg.de)

R. Müller, Institute for Stratospheric Chemistry, Science Department Jülich GmbH, D-52425 Jülich, Germany. (e-mail: ro.mueller@kfa-juelich.de)

M. P. Scheele, Royal Netherlands Meteorological Institute, P. O. Box 201, 3702 AE De Bilt, Netherlands. (e-mail: scheele@knmi.nl)

(Received April 30, 1996; revised December 17, 1996; accepted December 18, 1996.)